Design and Development of a 28 GHz Nb_3Sn ECR Ion Source Superconducting Magnet

Tengming Shen, *Senior Member, IEEE*, Ye Yang, Ray Hafalia Jr., Mariusz Juchno, Andy Lin, *Member, IEEE*, Jean-Francois Croteau, Hugh Higley, Mike Naus, Ian Pong, *Senior Member, IEEE*, Jose Ferradas Troitino, Paolo Ferracin, *Senior Member, IEEE*, Soren Prestemon, *Senior Member, IEEE*, Yoonhyuck Choi, Junwei Guo, Xiaoji Du, Danlu Zhang, Tomofumi Maruta, Guillaume Machicoane, Ting Xu, Jie Wei, and Jun Lu

***Abstract*—Worldwide several electron cyclotron resonance (ECR) ion sources have been developed and in operation for heavy ion accelerators using Nb-Ti superconducting magnets. The Versatile ECR ion source for NUclear Science (VENUS) at the Lawrence Berkeley National Lab (LBNL) and the newly commissioned 28 GHz superconducting ECR ion source at the Facility for Rare Isotope Beams (FRIB) were developed by LBNL. Both sources adopt a scheme with a sextupole magnet inside a mirror-type solenoid to confine the ions and electrons. Nb-Ti coils limit all the existing ECR ion sources to operate below ∼9 T at 4.2 K. Nb_3Sn potentially enables next generation ECR ion sources with a higher field limit (∼22 T at 4.2 K). As an example, a 45 GHz ECR ion source Nb_3Sn magnet is currently being developed by the Institute of Modern Physics (IMP) in China. Clearly conductor characteristics of Nb_3Sn are very much different and new development are needed to meet challenges such as coil fabrication. FRIB and LBNL team up again to develop ECR ion sources based on Nb_3Sn. Here as the first step, this paper describes the design of a second 28 GHz superconducting ECR ion source using Nb_3Sn coils at FRIB. We present conductor selection and characteristics, magnetic design, mechanical design and cold mass assembly, coil fabrication challenges and potential solution, quench protection, and the development and prototyping efforts so far.**

***Index Terms*—Electron cyclotron resonance, ion source, Nb_3Sn, superconducting magnet.**

I. Introduction

HIGH frequency Electron Cyclotron Resonance Ion Source (ECRIS) generates intense highly charged ion beams. An ECIRS uses a radial field supplied by six sextupole coils and mirrored axial fields from three solenoids (injection, middle and extraction) to confine the plasma [1]. The magnetic field for ECR is proportional to RF frequency as $B_{ECR}[\mathrm{T}] = f\,[\mathrm{GHz}]/28\,[\mathrm{GHz}]$, and the high radial field ($B_r \sim 2B_{ECR}$) and axial mirrored field ($B_{inj} \sim 4B_{ECR}$,$B_{\text{mid}} \sim 0.6B_{ECR}$, $B_{ext} \sim 2B_{ECR}$) are needed for high charge state ECRIS [2] [3]. Using the Nb-Ti technology, the 28 GHz ECRIS has been developed in many facilities, such as the VENUS at the Lawrence Berkeley National Lab (LBNL) [3] and the one at the Facility for Rare Isotope Beams (FRIB) of Michigan State University (MSU) [4]. Both of them adopted a sextupole-in-solenoid configuration.

For the current sextupole-in-solenoid based 28 GHz ECRISs, the peak field on the conductor is about 6–7 T, and it still can be achieved by Nb-Ti. However, regarding to the ECRIS greater than 40 GHz, the peak field increases to 10 T, which exceeds the critical field of Nb-Ti wires at the liquid helium temperature [5], [6], [7]. The conductor must be replaced by one that has a higher critical magnetic field. Thanks to the development of high field superconducting magnets for high luminosity LHC [8], Nb_3Sn is an excellent choice for the next-generation ECRIS from the point of view of the technology maturity. The non-Cu critical current density of Nb_3Sn wire can achieve ∼3000 A/mm ^{2} at 4.2 K, 12 T by the restacked-rod-process (RRP) method [9], [10]. However, unlike Nb-Ti, Nb_3 Sn is brittle and strain sensitive. Since the critical current degradation of Rutherford cables fabricated from RRP Nb_3Sn strands starts from a transverse pressure of ∼150–200 MPa at 4.2 K [11] and ∼100–120 MPa at room temperature, the coil stress must be managed so that there is no degradation occurred during the preload, cool down and energization. In addition to stress management, Nb_3Sn coil experiences dimensional changes during the reaction, adding complexity to coil fabrication and magnet assembly [8].

To establish the technology and investigate the feasibility for the next-generation high frequency ECRIS using the Nb_3Sn conductor, as a first step, a new 28 GHz ECRIS is currently under development at LBNL and FRIB. This ECRIS has a magnetic design identical to the one currently operated at FRIB [12], but the conductor of the sextupole coils switches to Nb_3Sn. After the Nb_3Sn coil fabrication technology is established, the feasibility of a Nb_3Sn-based, >45 GHz ECRIS will be explored for the next

Manuscript received 25 September 2023; revised 22 November 2023; accepted 27 November 2023. Date of publication 26 January 2024; date of current version 14 February 2024. This work was supported by the U.S. Department of Energy, Office of Science, Office of Nuclear Physics under the Cooperative Agreement DE-SC0000661. The work was supported by the U.S. Department of Energy (DOE), Office of Science at LBNL under Grant DE-AC02-05CH11231. *(Corresponding author: Tengming Shen.)*

Tengming Shen, Ye Yang, Ray Hafalia Jr., Mariusz Juchno, Andy Lin, Jean-Francois Croteau, Hugh Higley, Mike Naus, Ian Pong, Jose Ferradas Troitino, Paolo Ferracin, and Soren Prestemon are with Lawrence Berkeley National Laboratory (LBNL), Berkeley, CA 94720 USA (e-mail: tshen@lbl.gov).

Yoonhyuck Choi, Junwei Guo, Xiaoji Du, Danlu Zhang, Tomofumi Maruta, Guillaume Machicoane, Ting Xu, and Jie Wei are with the Facility for Rare Isotope Beams (FRIB), Michigan State University, East Lansing, MI 48824 USA.

Jun Lu is with National High Magnetic Field Laboratory (NHMFL), Tallahassee, FL 32210 USA.

Color versions of one or more figures in this article are available at https://doi.org/10.1109/TASC.2024.3358767.

Digital Object Identifier 10.1109/TASC.2024.3358767

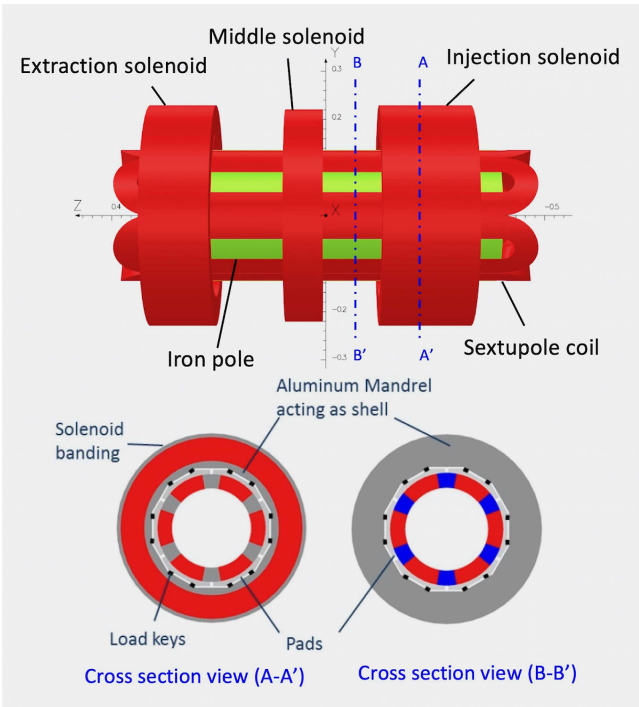

Fig. 1. Cross sectional view of the 28 GHz ECRIS superconducting magnet.

TABLE I
COIL DESIGN PARAMETERS

Item	Unit	Injection	Middle	Extraction	Sextupole
Inner radius	mm	170	170	170	100
Outer radius	mm	229.5	221.0	229.5	136.9
Length	mm	190.5	78.3	136.1	896.1
Turns	-	112×56	46×48	80×56	317
Nominal current	A	233	–155	152	924
Peak field	T	6.2	3.4	4.1	6.7
Conductor	-	Nb-Ti	Nb-Ti	Nb-Ti	Nb_3Sn

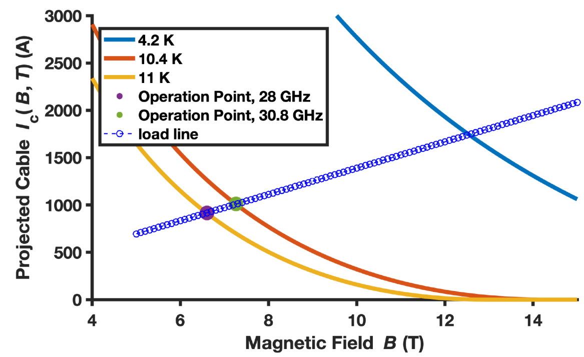

Fig. 2. Load line for the Nb_3Sn sextupole coil operated at 28 GHz and 30.8 GHz. The cable I_c was projected using a minimum strand I_c(4.2 K and 12 T) of 299 A. The effect of self-field is excluded.

step. In this paper, we present Nb_3Sn conductor selection and characteristics, magnetic design, mechanical design and cold mass assembly, coil fabrication challenges and potential solution, quench protection, and the development and prototyping efforts so far.

II. Overall System Design and Nb_3Sn Conductor

A. Superconducting Magnet System

The magnetic design for the new 28 GHz ECRIS is identical to the one currently operated at FRIB besides the Nb_3Sn sextupole coil. As presented in Fig. 1, three solenoids, injection, middle and extraction coils, generate the axial injection field of 4 T, minimum field of 0.4 T and extraction field of 3 T at the magnet center axis. The sextupole coil with the iron pole provides a maximum radial field of 2.07 T at the plasma chamber wall at a radius of 71.85 mm. The mechanical structure and the magnet assembly resemble the general scheme established for the existing FRIB ECRIS Nb-Ti magnet using a bladder-and-key method [13]. The Nb-Ti solenoid coils are wound on an aluminum mandrel with external bands. Each Nb_3Sn sextupole coil is wound around its pole, reacted and then impregnated. After impregnation, six of them will be assembled using the load pads and inserted into the aluminum mandrel of the solenoid. The mandrel acts as a shell to apply the preload on the sextupole after the cool down. Table I lists the coil design parameters. The Nb_3Sn sextupole coils are redesigned with the nominal current of 924 A (28 GHz) and 317 turns per pole. The peak fields on the conductor are 6.7 T and 7.3 T at 28 GHz and 30.8 GHz, respectively. As shown in Fig. 2, the nominal operation point at the 28 GHz is 54% of the short sample limit on the load line and has a temperature margin of 6.8 K by using the Nb_3Sn conductor. Even for a operation point higher than 10 T, it still has a lot of margin to the critical surface at 4.2 K.

TABLE II
WIRE AND CABLE SPECIFICATION FOR THE ECRIS SUPERCONDUCTING MAGNET

Item	Unit	Value
Superconducting cable:		
Cable dimension (bare)	mm^2	2.35×1.25
Cable dimension (insulated)	mm^2	2.60×1.55
Insulation	-	S-2 glass, 2-ply, QXF type
Cable pitch angle	degree	22
Number of strands	-	6
Strand:		
Diameter	mm	0.7
Wire design	-	RRP® 60/91 (Nb:Sn = 3.6:1)
Subelement number	-	60
Subelement diameter, d_s	μm	56
Cu:non-Cu	-	>1.6
Twist pitch	mm	19
RRR	-	>100
Minimum non-Cu J_c	A/mm^2	2180 (12 T, 4 K)

B. RRP Nb_3Sn Sexutupole Coil Conductor

Table II lists the specifications of the conductor selected for the sextupole coil. The final conductor is a Rutherford cable made with six ϕ0.7 mm RRP 60/91 strands, and insulated with

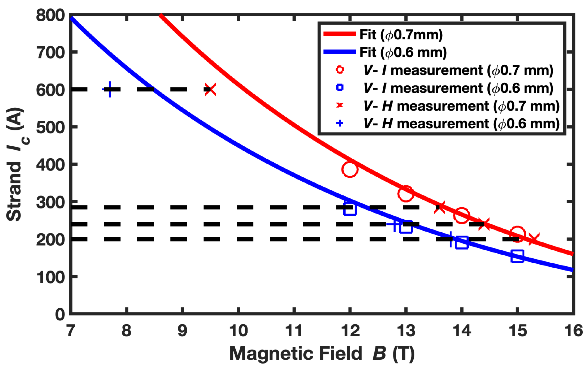

Fig. 3. Measured critical current and field for ϕ0.6 mm and ϕ0.7 mm strands at 4.2 K. Strands were 15% rolled. The hollow dots are the critical current measured at the specific magnetic field. The line indicates the general fit referred from [15]. The dashed lines indicate that the strands are able to carry the transport currents (200 A, 240 A, 280 A, and 600 A) during field sweeps to the magnetic fields marked with + and × dots.

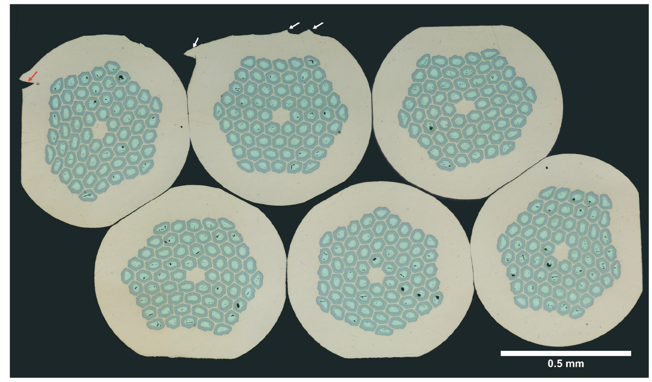

Fig. 4. Optical micrograph of the Rutherford cable cross section fabricated at LBNL. Red and white arrows show marking added to two wires before metallographic preparation for identification of the spool of origin of each strand during cable cross-section analysis.

the braided S-2 glass. Round RRP strands were selected over fine-filament, bronze-route, rectangular strands due to its field reach provided by its high critical current density, flexibility of setting its Cu-to-nonCu ratio, and the ability of turning the strand into a rectangular conductor with a Rutherford cable.

A concern is the low-field magnetic instability of the Nb_3Sn strands. The selected RRP 60/91 strand was modified from the conventional RRP 84/91 strand architecture by removing the outside 24 sub-elements to increase the Cu:non-Cu ratio to 1.6 from 0.85–1.1 to enhance the stability of the strands against flux jumps. The selected strands have a reduced Sn design and the heat treatment is selected as 665 °C for 50 h to avoid the degradation of *RRR* and the strain cliff. Fig. 3 presents the critical current measured at each magnetic field (*V-I* measurement) and results of a stability current measurement (*V-H* measurement at a constant current). During the *V-H* measurement, the voltage spikes were found below 1 T during the sweep of magnetic field and are attributed to flux jumps. Since the magnetic stability can be improved by reducing the sub-element diameter [14], the ϕ0.7 mm ($d_s \sim 56$ μm) RRP 60/91 wire was drawn down to ϕ0.6 mm ($d_s \sim 48$ μm) and diameter and it was also tested. For a transport current of 600 A, the upper critical field was determined at 4.2 K to be 7.7 T and 9.5 T for ϕ0.6 mm and ϕ0.7 mm strands respectively. No quench were observed for a transport current of 600 A for both ϕ0.6 mm and ϕ0.7 mm strands (both were 15% rolled) up to to 7.5 T and 9.2 T, respectively. Thus, both strands have good magnetic stability. The ϕ0.7 mm RRP 60/91 strand is selected for the cable.

C. Cable Fabrication

A total of 790 m cable was fabricated at LBNL and insulated. The *RRR* of the kink section of strands extracted from the cable showed a *RRR* of greater than 500. Fig. 4 shows the optical micrograph of the Rutherford cable fabricated for the sextupole coil. The local deformation of the sub-elements for the edge strands was deemed to be acceptable.

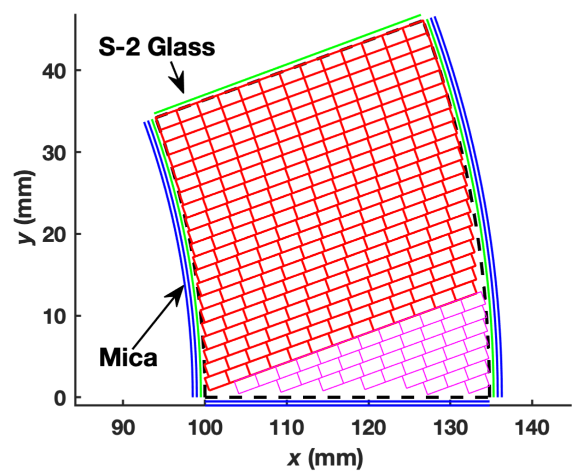

Fig. 5. Cross-sectional view of the Nb_3Sn sextupole coil winding. The coil winding starts from the upper left side around the iron pole and finishes at the middle plane. First 21 layers have 13 turns in each layer (red), and the rest of 7 layers has 44 in total (pink). The conductor is assumed to expand 3.25% along the width of the cable and 4% along the thickness of the cable. The winding filling factor is assumed to be 89% with cable expansions due to reaction taken into consideration.

III. Sextupole Coil Fabrication Plan

A key challenge to Nb_3Sn magnets is the coil fabrication. Each sextupole coil is a cosine-theta type coil wound around an iron pole with the rectangular Nb_3Sn cable. A significant difference from those AUP type Nb_3Sn coils is the much larger number of turns per coil. The cross-section of the sextupole coil winding after the reaction is represented in Fig. 5. The leads are routed in and out at the mid-plane of the coil; the first 21 layers are aligned on the inner radius, and the rest of them are aligned to the outer radius to achieve the total turns of 317. After the winding, S-2 glass fiber insulation and MICA sheets are placed to protect the coil, and the aluminum bronze end-shoes are installed to constrain the end turns and leads. Then, each individual sextupole coil is transfered to a stainless steep reaction tooling for reaction. MICA sheets allow cables to move against tooling during reaction. The Nb_3Sn coils feature

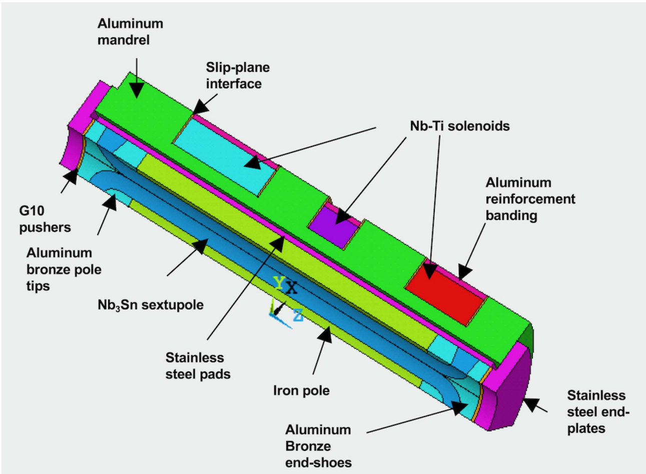

Fig. 6. 60-degree symmetric model used in ANSYS for the mechanical analysis.

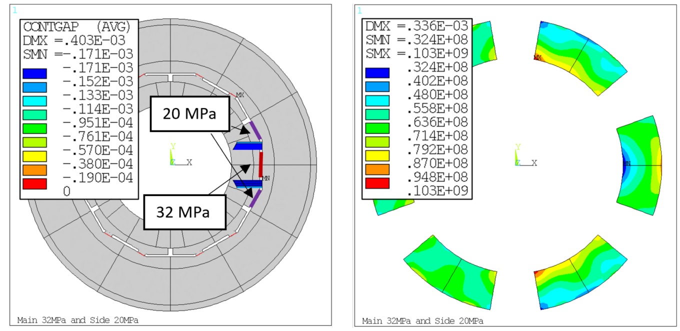

Fig. 7. Calculated Von Mises stress in the Nb_3Sn sextupole coil after two additional keys are inserted with a pressure 20 MPa. Only single bladder (red bar) is applied for the original design.

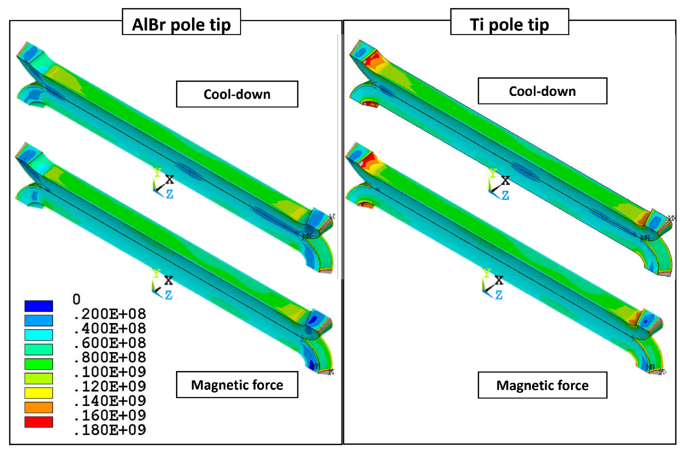

Fig. 8. Von Mises stress in the Nb_3Sn sextupole coil after cool-down and energization. The left plots indicate the case using the aluminum bronze pole tip; the right one indicate the case using the titanium pole tip.

dimensional changes during the reaction, which could cause the degradation of the cable or damage on the insulation [16]. To avoid degradation during the coil fabrication, an axial gap between two split iron poles is introduced to release the tension on cable [17]. A prototype of a full-length sextupole coil is being fabricated to investigate the coil fabrication technique and verify tooling designs. It will be tested in a mirror coil configuration.

IV. Mechanical Analysis and Assembly

The maximum stress in the Nb_3Sn coil must be kept lower than 150 MPa at cryogenic temperature and 100 MPa at room temperature to avoid the degradation. The mechanical analysis is carried out to optimize the stress during the assembly and energization.

A. Stress During the Assembly

Fig. 6 presents a symmetric model in ANSYS for the mechanical analysis. Stresses at each step of solenoid winding, key insertion, cooling down and energization are investigated. The solenoid winding tension and aluminum banding are set as 60 MPa and 30 MPa, respectively. During the assembly, the experience with the FRIB Nb-Ti ECR magnet is that the coils are overloaded by a factor of three in order to insert loading keys due to nonuniform deformation of the mandrel caused by solenoid winding. However the peak Von Mises stress in the sextupole coil becomes 122 MPa during bladder operation. In order to minimize the stress, a potential solution is to add two bladders provide a more uniform loading. As plotted in Fig. 7, the Von Mises stress in the sextupole coil is mitigated to an acceptable value of 103 MPa.

B. Stress After Cool-Down and Energization

The sextupole coil after cool-down and energization also shows the high stress about 180 MPa at the pole tips for the Nb-Ti coil design (see Fig. 8). To reduce the stress in the sextupole coil, the titanium pole tips are replaced by one made of aluminum bronze, which has a high thermal expansion coefficient. As the result, the aluminum bronze pole tip gives a lower stress of $<$140 MPa in the sextupole coil.

V. Quench Protection

The quench protection of the VENUS and FRIB 28 GHz Nb-Ti magnets is passive with cold diodes. For Nb_3Sn sextupole coils, active protection with a room temperature dump resistor is selected. Different to Nb-Ti, a difficulty for protecting a Nb_3Sn coil is the quench detection due to the flux jump voltage. The flux jump generates a high voltage in the order of 100 mV with a long time interval, which ranges from 10–20 ms in [18] and to 150 ms in IMP's 45 GHz Nb_3Sn magnet [19]. In order to reduce the error detection, the discrimination time window will be extended for the quench detection. Fig. 9 shows the current decay and temperature rise for 28 GHz operation with a long discrimination time of 200 ms. The calculation was accomplished using the QUENCH code [14]. The operation current is 924 A and the inductance is 0.42 H; the required time constant for current decay is about 0.92 s with the maximum temperature of 300 K and thus a dump resistor of 0.458 O is required. The maximum temperature and voltage are also confirmed to be $<$350 K and $<$450 V. The dump resistor is ground at the mid-tap to limit the electric voltage to ground to $<$225 V. The coil internal voltage is low due to low normal zone propagation velocity of $<$0.8 m/s

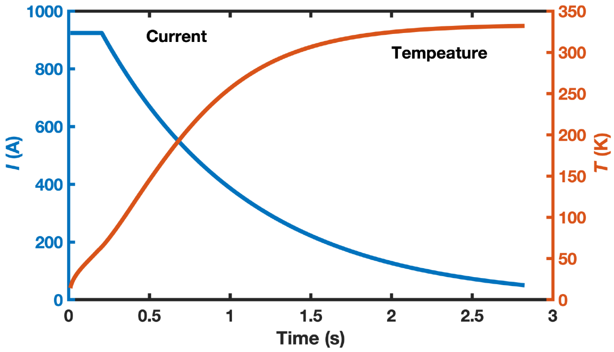

Fig. 9. Nb_3Sn sextupole coil current decay and hot spot temperature at 28 GHz operation with a discrimination time of 200 ms for quench detection. It was protected with a dump resistor of 0.46 O.

along the axial direction of the conductor. If the discrimination time is reduced to 50 ms, the hot spot temperature would drop to 200 K.

VI. Conclusion

The development of a next-generation, 28 GHz Nb_3Sn based ECRIS is ongoing, leveraging the design and construction experience of the Nb-Ti ECRIS superconducting magnet currently operated at the FRIB. Various aspects of using Nb_3Sn to construct a cosine-theta sextupole coil suitable for an ECRIS have been discussed, including magnetic instabilities, coil fabrication, stress management during magnet assembly, cool-down, and energization, and quench protection, and our technical choices are described. Conductor has been selected, characterized, and the results meet design requirements. The cable has been fabricated for the prototype coil. Currently, coil winding is ongoing with tooling fabrication, with the goal of testing a full-length prototype coil in a mirror magnet structure as the vehicle for technology development. The mirror magnet will be followed with the construction of the entire magnet.

Acknowledgment

The authors thank William Hassenzahl for assistance with using the QUENCH program, Helene Felice with CEA Saclay, Alfred Nobrega with Fermialb, and Diego Arbelaez with LBNL for technical review of this project, and Etienne Rochepault for his efforts with developing various tools for designing and analyzing the FRIB ECRIS Nb-Ti magnet, which remain useful for this project. We also thank Elizabeth Lee, Algirdas Baskys, Elaine Burron and Mike Gronley, all with LBNL, for assistance with cable fabrication.

References

[1] C. Lyneis et al., "Fourth generation electron cyclotron resonance ion sources," *Rev. Sci. Instruments*, vol. 79, no. 2, Feb. 2008, Art. no. 02A321, doi: 10.1063/1.2816793.
[2] D. Hitz et al., "Results and interpretation of high frequency experiments at 28 GHz in ECR ion sources, future prospects," *Rev. Sci. Instruments*, vol. 73, no. 2, pp. 509–512, Feb. 2002, doi: 10.1063/1.1429313.
[3] C. Taylor et al., "Magnet system for an ECR ion source," *IEEE Trans. Appl. Supercond.*, vol. 10, no. 1, pp. 224–227, Mar. 2000, doi: 10.1109/77.828215.
[4] D. Arbelaez et al., "Test results for a superconducting 28-GHz ion source magnet for FRIB," *IEEE Trans. Appl. Supercond.*, vol. 29, no. 5, Jun. 2015, Art. no. 4100605.
[5] P. Ferracin et al., "Nb_3Sn superconducting magnets for electron cyclotron resonance ion sources," *Rev. Sci. Instruments*, vol. 81, no. 2, Feb. 2010, Art. no. 02A309.
[6] M. Juchno et al., "Mechanical design of a Nb_3Sn superconducting magnet system for a 45GHz ECR ion source," *IEEE Trans. Appl. Supercond.*, vol. 28, no. 3, Apr. 2018, Art. no. 4602806, doi: 10.1109/TASC.2017.2773832.
[7] S. Prestemon et al., "Design of a Nb_3Sn magnet for a 4th generation ECR ion source," *IEEE Trans. Appl. Supercond.*, vol. 19, no. 3, pp. 1336–1339, Jun. 2009, doi: 10.1109/TASC.2009.2017719.
[8] E. Todesco et al., "The high luminosity LHC interaction region magnets towards series production," *Supercond. Sci. Tech.*, vol. 34, no. 5, Mar. 2021, Art. no. 053001, doi: 10.1088/1361-6668/abdba4.
[9] J. Parrell et al., "High field Nb_3Sn conductor development at Oxford Superconducting Technology," *IEEE Trans. Appl. Supercond.*, vol. 13, no. 2, pp. 3470–3473, Jun. 2003, doi: 10.1109/TASC.2003.812360.
[10] X. Xu, "A review and prospects for Nb_3Sn superconductor development," *Supercond. Sci. Tech.*, vol. 30, no. 9, Aug. 2017, Art. no. 093001, doi: 10.1088/1361-6668/aa7976.
[11] P. Ebermann et al., "Irreversible degradation of Nb_3Sn Rutherford cables due to transverse compressive stress at room temperature," *Supercond. Sci. Tech.*, vol. 31, no. 6, May 2018, Art. no. 065009, doi: 10.1088/1361-6668/aab5fa.
[12] H. Felice et al., "Design of a superconducting 28 GHz ion source magnet for FRIB using a shell-based support structure," *IEEE Trans. Appl. Supercond.*, vol. 25, no. 3, Jun. 2015, Art. no. 4101405, doi: 10.1109/TASC.2014.2377730.
[13] S. Caspi et al., "The use of pressurized bladders for stress control of superconducting magnets," *IEEE Trans. Appl. Supercond.*, vol. 11, no. 1, pp. 2272–2275, Mar. 2001, doi: 10.1109/77.920313.
[14] M. Wilson, *Superconducting Magnets*. New York, NY, USA: Oxford Univ. Press, 1983.
[15] J. Van Nugteren, "High temperature superconductor accelerator magnets," Ph.D. dissertation, University of Twente, The Netherlands, 2016.
[16] M. Durante et al., "Geometrical behavior of Nb_3Sn Rutherford cables during heat treatment," *IEEE Trans. Appl. Supercond.*, vol. 26, no. 4, Jun. 2016, Art. no. 4802705, doi: 10.1109/TASC.2016.2530166.
[17] H. Felice et al., "Impact of coil compaction on Nb_3Sn LARP HQ magnet," *IEEE Trans. Appl. Supercond.*, vol. 22, no. 3, Jun. 2012, Art. no. 4001904, doi: 10.1109/TASC.2012.2183843.
[18] A. Lietzke et al., "Differentiation of performance-limiting voltage transients during Nb_3Sn magnet testing," *AIP Conf. Proc.*, vol. 824, no. 1, pp. 550–557, Mar. 2006, doi: 10.1063/1.2192394.
[19] L. Sun et al., "Progress on the development of key technologies for the fourth generation ECR ion source FECR," *J. Phys.: Conf. Ser.*, vol. 2244, no. 1, Apr. 2022, Art. no. 012021, doi: 10.1088/1742-6596/2244/1/012021.